Predicting speciation of Ammonia, MEA and DEA using only the ionic radius and the ionic charge

Marcus C. Simoes, Kevin J. Hughes*, Derek B. Ingham, Lin Ma, Mohamed Pourkashanian

Energy-2050, Department of Mechanical Engineering, University of Sheffield, Sheffield S10 2TN, United Kingdom.

ABSTRACT: This study investigates the speciation of CO_2 involving the most common solvents used to capture carbon from the flue gas, i.e. ammonia, MEA and DEA. This requires the knowledge of both the activity coefficients of the species involved and the equilibrium constants of the relevant reactions. In contrast to the equilibrium constants, which can be obtained from the literature, the activity coefficients of the aqueous species are required to be estimated. Normally, semi-empirical models are used to estimate these activity coefficients, i.e. equations that contain unknown parameters that are obtained through regression against experimental data. In contrast, in this study the activity coefficients are predicted using equations that require only the knowledge of the ionic radii and charges of the species involved in the equilibrium. As a conclusion, the model developed shows a very good agreement with the experimental data obtained, either from spectroscopy or from Vapor Liquid Equilibrium (VLE), up to a solvent mass fraction of 20%.

INTRODUCTION

The increase of the CO_2 levels in the atmosphere significantly contributes to an increase in the global temperatures. Moreover, climate change can impose several threats to humanity, such as risks to unique and threatened systems, extreme weather events that can cause breakdown of the infrastructure and critical services such as electricity, water supply, food insecurity, etc[1]. Therefore, it is important to find options to tackle these CO_2 emissions. In this context, one of the most important options available is the carbon capture and storage (CCS) using chemical solvents, such as ammonia and several types of amines, including the alkanolamines MEA, DEA, MDEA, etc. Therefore, understanding and modelling the chemistry related to these chemical solvents is highly important.

Several models describing the equilibrium involving ammonia-based solvents[2–10] and alkanolamine-based solvents[11–21] can be found in the literature. A common feature of all of these models is that they use semi-empirical equations to estimate the activity coefficients of the species, and these equations contain parameters that can only be obtained through regression against experimental data, normally VLE experimental data. Thus, these models are not predictive, since normally they cannot be used to estimate the equilibrium beyond the range in which experimental data are available. In contrast, this study uses expressions developed previously[22] to calculate the activity coefficients, and these expressions require only the knowledge of the properties of the solutions. In particular, these expressions correlate the second virial coefficients in the Pitzer equations $B_{MX}^{(0)}$ and $B_{MX}^{(1)}$ with the ionic radii and the charges of the species involved in the equilibrium, which are in general known properties. Nevertheless, if a given ionic radius is not tabulated in the literature, it can be estimate using a model developed in another previous study,[23]

3

which presents a formulation to calculate the ionic radius of complex ions using the sizes of their individual components.

EQUILIBRIUM MODEL

The equilibrium model developed in this study is based on (i) the chemical equilibrium in the aqueous phase, (ii) the phase equilibrium, (iii) the electroneutrality principle, and (iv) the mass balance of the species.

Chemical Equilibrium in the Aqueous Phase

A series of reactions occurs during the CO_2 absorption in aqueous ammonia/amine, as follows:[5,12]

Dissolution of CO_2 into the aqueous phase:

$$CO_{2(g)} \overset{H_1}{\leftrightarrow} CO_{2(l)} \tag{1}$$

Dissolution of amine/ammonia into the aqueous phase:[5,13]

$$NH_{3(g)} \overset{H_{2a}}{\longleftrightarrow} NH_{3(l)} \tag{2a}$$

$$Amine_{(g)} \overset{H_{2b}}{\longleftrightarrow} Amine_{(l)} \tag{2b}$$

Water Dissociation:

$$H_2O_{(l)} \overset{K_1}{\leftrightarrow} H^+_{(aq)} + OH^-_{(aq)} \tag{3}$$

Carbon dioxide ionization:

$$CO_{2(aq)} + H_2O_{(l)} \overset{K_2}{\leftrightarrow} HCO^-_{3(aq)} + H^+_{(aq)} \tag{4}$$

Bicarbonate ionization:

$$HCO^-_{3(aq)} \overset{K_3}{\leftrightarrow} CO^{2-}_{3(aq)} + H^+_{(aq)} \tag{5}$$

Amine/ammonia protonation:

$$\text{Amine}_{(aq)} + \text{H}^+_{(l)} \overset{K_{4a}}{\longleftrightarrow} \text{AmineH}^+_{(aq)} \tag{6a}$$

$$\text{NH}_{3(aq)} + \text{H}_2\text{O}_{(l)} \overset{K_{4b}}{\longleftrightarrow} \text{NH}^+_{4(aq)} + \text{OH}^-_{(aq)} \tag{6b}$$

Amine/ammonia carbamate hydrolysis

$$\text{AmineCOO}^-_{(aq)} + \text{H}_2\text{O}_{(l)} \overset{K_{5a}}{\longleftrightarrow} \text{Amine}_{(aq)} + \text{HCO}^-_{3(aq)} \tag{7a}$$

$$\text{NH}_2\text{COO}^-_{(aq)} + \text{H}_2\text{O}_{(l)} \overset{K_{5b}}{\longleftrightarrow} \text{NH}_{3(aq)} + \text{HCO}^-_{3(aq)} \tag{7b}$$
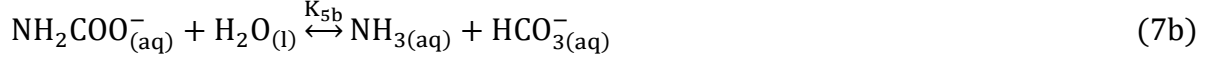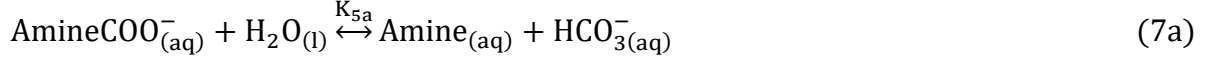
The equilibrium constants of the reactions represented by Equations (3) to (7) are given as follows:

$$K_1 = [\text{H}^+][\text{OH}^-]\frac{\gamma_{\text{H}^+}\gamma_{\text{OH}^-}}{a_{\text{H}_2\text{O}}} \tag{8}$$

$$K_2 = \frac{[\text{H}^+][\text{HCO}_3^-]}{[\text{CO}_2]}\frac{\gamma_{\text{H}^+}\gamma_{\text{HCO}_3^-}}{\gamma_{\text{CO}_2}a_{\text{H}_2\text{O}}} \tag{9}$$

$$K_3 = \frac{[\text{H}^+][\text{CO}_3^{2-}]}{[\text{HCO}_3^-]}\frac{\gamma_{\text{H}^+}\gamma_{\text{CO}_3^{2-}}}{\gamma_{\text{HCO}_3^-}} \tag{10}$$

$$K_{4a} = \frac{[\text{AmineH}^+]}{[\text{Amine}][\text{H}^+]}\frac{\gamma_{\text{AmineH}^+}}{\gamma_{\text{Amine}}\gamma_{\text{H}^+}} \tag{11a}$$

$$K_{4b} = \frac{[\text{NH}_4^+][\text{OH}^-]}{[\text{NH}_3]}\frac{\gamma_{\text{NH}_4^+}\gamma_{\text{OH}^-}}{\gamma_{\text{NH}_3}a_{\text{H}_2\text{O}}} \tag{11b}$$

$$K_{5a} = \frac{[\text{Amine}][\text{HCO}_3^-]}{[\text{AmineCOO}^-]}\frac{\gamma_{\text{Amine}}\gamma_{\text{HCO}_3^-}}{\gamma_{\text{AmineCOO}^-}} \tag{12a}$$

$$K_{5b} = \frac{\text{NH}_2\text{COOH}^-}{[\text{NH}_3][\text{HCO}_3^-]}\frac{\gamma_{\text{NH}_2\text{COOH}^-}a_{\text{H}_2\text{O}}}{\gamma_{\text{NH}_3}\gamma_{\text{HCO}_3^-}} \tag{12b}$$

In terms of equilibrium constants, these were taken from the literature and are shown in Table 1. In addition, the temperature dependence of these equilibrium constants is expressed as follows:[5]

$$\ln K_i = A_{1,i} + \frac{A_{2,i}}{T} + A_{3,i}\ln T + A_{4,i}T \tag{13}$$

Table 1. Temperature dependence of the Equilibrium Constants involving the NH_3-CO_2-H_2O, MEA-CO_2-H_2O and DEA-CO_2-H_2O systems: $\ln K_i = A_{1,i} + \frac{A_{2,i}}{T} + A_{3,i} \ln T + A_{4,i}T$.

Reaction / Constant Equation	$A_{1,i}$	$A_{2,i}$	$A_{3,i}$	$A_{4,i}$	Ref.
$H_2O_{(l)} \overset{K_1}{\leftrightarrow} H^+_{(aq)} + OH^-_{(aq)}$	1.409×10^2	-1.345×10^4	-2.248×10^1		5
$CO_{2(aq)} + H_2O_{(l)} \overset{K_2}{\leftrightarrow} HCO^-_{3(aq)} + H^+_{(aq)}$	1.023×10^2	-7.726×10^3	-1.451×10^1	-2.798×10^{-2}	5
$HCO^-_{3(aq)} \overset{K_3}{\leftrightarrow} CO^{2-}_{3(aq)} + H^+_{(aq)}$	1.167×10^2	-9.137×10^3	-1.811×10^1	-2.246×10^{-2}	5
$MEA_{(aq)} + H^+_{(l)} \overset{K_{4a,MEA}}{\longleftrightarrow} MEAH^+_{(aq)}$	-7.996×10^{-1}	8.095×10^3		7.484×10^{-3}	13
$MEACOO^-_{(aq)} + H_2O_{(l)} \overset{K_{5a,MEA}}{\longleftrightarrow} MEA_{(aq)} + HCO^-_{3(aq)}$	2.890×10^0	-3.635×10^3			13
$DEA_{(aq)} + H^+_{(l)} \overset{K_{4a,DEA}}{\longleftrightarrow} DEAH^+_{(aq)}$	-6.794×10^0	-5.928×10^3			24
$DEACOO^-_{(aq)} + H_2O_{(l)} \overset{K_{5a,DEA}}{\longleftrightarrow} DEA_{(aq)} + HCO^-_{3(aq)}$	4.515×10^0	-3.417×10^3			24
$NH_{3(aq)} + H_2O_{(l)} \overset{K_{4b}}{\leftrightarrow} NH^+_{4(aq)} + OH^-_{(aq)}$	9.797×10^1	-5.914×10^3	-1.506×10^1	-1.101×10^{-2}	5
$NH_2COO^-_{(aq)} + H_2O_{(l)} \overset{K_{5b}}{\leftrightarrow} NH_{3(aq)} + HCO^-_{3(aq)}$	2.015×10^1	6.041×10^2	-4.017×10^0	5.031×10^{-3}	5

In terms of the activity coefficients, the Pitzer model[25–29] was selected to estimate these properties, and the relevant equations are presented elsewhere.[30] Considering these equations, apart from $B^{(0)}_{MX}$ and $B^{(1)}_{MX}$, all the other parameters describing interactions between ionic species are set to zero. Normally $B^{(0)}_{MX}$ and $B^{(1)}_{MX}$ are treated as empirical parameters. In contrast, as mentioned in the introduction, in this study $B^{(0)}_{MX}$ and $B^{(1)}_{MX}$ are not treated as empirical parameters. Instead, expressions that correlate these parameters with the ionic radii and charges[22] are used, and these expressions are as follows:

$$B^{(0)}_{MX} = \alpha_1 z_M^{1.62} z_X^{-1.35} |r_M - 1.5 r_X|^{1.2} + \alpha_2 \qquad (14)$$

$$B_{MX}^{(1)} = \alpha_3 z_X^{-0.4} \left(z_M^2 z_X^{0.6}(1 + |r_M - 1.2r_X|^{0.2}) \right)^2 + \alpha_4 z_M^2 z_X^{0.2}(1 + |r_M - 1.2r_X|^{0.2}) + \alpha_5 z_X^{-0.4}$$

(15)

where $\alpha_1 = 0.04432$, $\alpha_2 = 0.05758$, $\alpha_3 = 0.01001$, $\alpha_4 = 0.12017$ and $\alpha_5 = 0.05226$.

Some of the species considered in this study, e.g. $MEACOO^-$ and $DEACOO^-$ have unknown ionic radii, but they can be estimated using expressions developed in a previous study,[23] as follows:

$$r_X = z_X^{\varepsilon_1} \left(\sum_j v_j r_{M_j}^3 + \sum_k v_k r_{X_k}^3 \right)^{1/3}$$

(16)

$$r_M = z_M^{\varepsilon_2} \kappa_1 \left(\sum_j v_j r'_{M_j}^{\varepsilon_3} + \sum_k v_k r'_{X_k}^{\varepsilon_3} \right)^{1/3}$$

(17)

The value of the parameter ε_1 in Equation (16) is (0.057±0.005). Regarding the parameters in Equation (17), namely the constant κ_1 and the power parameters ε_2 and ε_3, these values are (1.249±0.013) Å^2, (-0.264±0.025) and (1.50±0.11), respectively.[23]

The estimated virial parameters $B_{MX}^{(0)}$ and $B_{MX}^{(1)}$ are shown in Table 2, along with the ionic radii considered in the calculations.

Table 2. Estimated virial parameters in the Pitzer equations for NH_3-CO_2-H_2O, MEA-CO_2-H_2O and DEA-CO_2-H_2O systems at 25 °C.

Species M,X	B^0_{MX} Estimated	B^1_{MX} Estimated	r_M (Å)	r_X (Å)	reference r_M	reference r_X
			NH_3-CO_2-H_2O			
H^+, HCO_3^-	0.1891	0.3552	0.30	1.85	31	32
NH_4^+, HCO_3^-	0.1180	0.3233	1.48	1.85	32	32
NH_4^+, OH^-	0.0776	0.2778	1.48	1.33	32	32
H^+, CO_3^{2-}	0.1065	0.4125	0.30	1.78	31	32
NH_4^+, CO_3^{2-}	0.0790	0.3687	1.48	1.78	32	32
H^+, NH_2COO^-	0.2494	0.3676	0.30	1.59	31	this study
NH_4^+, NH_2COO^-	0.1724	0.3456	1.48	1.59	32	this study
			MEA-CO_2-H_2O			
$MEAH^+$, HCO_3^-	0.0887	0.2882	1.60	1.85	this study	32
$MEAH^+$, OH^-	0.0584	0.3082	1.60	1.33	this study	32
$MEAH^+$, CO_3^{2-}	0.0678	0.3125	1.60	1.78	this study	32
H^+, $MEACOO^-$	0.2504	0.3678	0.30	1.61	31	this study
$MEAH^+$, $MEACOO^-$	0.1399	0.3305	1.60	1.61	this study	this study
			DEA-CO_2-H_2O			
$DEAH^+$, HCO_3^-	0.0748	0.2749	1.48	1.85	this study	32
$DEAH^+$, OH^-	0.0691	0.3227	1.48	1.33	this study	32
$DEAH^+$, CO_3^{2-}	0.0625	0.3272	1.48	1.78	this study	32
H^+, $DEACOO^-$	0.2699	0.3711	0.30	1.61	31	this study
$DEAH^+$, $DEACOO^-$	0.1396	0.3283	1.48	1.61	this study	this study

Vapor-Liquid Equilibrium (VLE)

The amines investigated in this study are highly soluble in water, and thus Equation (2b) can be disregarded for these amines. In contrast, ammonia is not as soluble in water as are the amines,

and hence Equation (2a) is required to be taken into consideration. The gas-liquid equilibrium involving CO_2 and NH_3 can be calculated using Henry's law,[12] as follows:

$$Py_i = H_{i,w}^{(m)} m_i \tag{18}$$

where $H_{i,w}^{(m)}$ is the Henry constant, which can be calculated as follows:

$$\ln H_{i,w} = D_{1,i} + \frac{D_{2,i}}{T} + D_{3,i}T + D_{4,i}\ln T + \frac{D_{5,i}}{T^2} \tag{19}$$

with the constants $D_{1,i}$ to $D_{5,i}$ being shown in Table 3.[33]

For water, the gas-liquid equation is given as follows:[2]

$$Py_w\, \varphi_w = f_w^0 a_w \tag{20}$$

where φ_w is the vapour phase fugacity coefficient, which can be calculated using the Redlich-Kwong equations,[34] a_w is the water activity, which can be calculated by the Pitzer equation[30] and f_w^0 is the fugacity of the liquid water, which can be calculated as follows:[35]

$$\ln f_w^0 \left(\frac{T}{K}\right) = 57.042 + \frac{-7004.8}{T} + 0.0035888T - 6.6689\ln(T) - 8.5054 \times 10^{-7}T^2 \tag{21}$$

Table 3. Parameters for the Henry's constant in MPa kg/mol:[33] $\ln H_{i,w} = D_{1,i} + \frac{D_{2,i}}{T} + D_{3,i}T + D_{4,i}\ln T + \frac{D_{5,i}}{T^2}$.

Compound	$D_{1,i}$	$D_{2,i}$	$D_{3,i}$	$D_{4,i}$	$D_{4,i}$	Ref.
NH_3	3.932×10^0	-1.879×10^3			-3.551×10^5	33
CO_2	1.929×10^2	-9.624×10^3	1.441×10^{-2}	-2.875×10^1		33

Electroneutrality Principle

The electroneutrality principle is based on the fact that the aqueous solutions as a whole have zero net charge.[36] On applying this principle to the NH_3-CO_2-H_2O system, the following equation is obtained:

$$m_{H^+} + m_{NH_4^+} - 2m_{CO_3^{2-}} - m_{HCO_3^-} - m_{OH^-} - m_{NH_2COO^-} = 0 \tag{22}$$

Likewise, if the electroneutrality principle is applied for the Amine-CO_2-H_2O system, the following equation is obtained:

$$m_{H^+} + m_{AmineH^+} - 2m_{CO_3^{2-}} - m_{HCO_3^-} - m_{OH^-} - m_{AmineCOO^-} = 0 \tag{23}$$

Mass Balance of the Species

Using the mass conservation principle, the following equations can be obtained for the NH_3-CO_2-H_2O system:

$$m_{CO_2\,initial} = m_{CO_3^{2-}} + m_{HCO_3^-} + m_{NH_2COO^-} + m_{CO_2} \tag{24}$$

$$m_{NH_3\,initial} = m_{NH_4^+} + m_{NH_2COO^-} + m_{NH_3} \tag{25}$$

Likewise, using the mass conservation principle, the following equations can be obtained for the Amine-CO_2-H_2O system:

$$m_{CO_2\,initial} = m_{CO_3^{2-}} + m_{HCO_3^-} + m_{MEACOO^-} + m_{CO_2} \tag{26}$$

$$m_{Amine_{initial}} = m_{AmineH^+} + m_{AmineCOO^-} + m_{Amine} \tag{27}$$

RESULTS

CO_2-NH_3-H_2O System

Table 4 shows a comparison between the calculated and the experimental values[37] obtained by ^{13}C NMR spectroscopy at 25 °C. As can be seen in this table, there is in general a very good agreement between the calculated values obtained through Equations (14) and (15) and the

experimental data.[37] However, it is important to note that at high concentrations this agreement slightly deteriorates. This is expected since at higher concentrations more terms are required to be added to the Pitzer equations, for instance to account for the interactions between triplets of ions, ion-neutral interactions, etc.

In terms of partial pressures, Figure 1 illustrates the agreement between the model and the VLE experimental data from the literature.[38] As can be seen in this figure, the agreement between calculated and experimental[38] partial pressures of CO_2 at various molalities of NH_3 at 20 °C is very good in general, but the accuracy decreases as the concentration increases. As explained above, this is because at higher concentrations more terms are required to be added to the Pitzer equations. In contrast, even at high concentrations, the model predicts very well the concentrations of NH_3, and this is probably because for the ammonia-containing species two virial parameters suffice to accurately describe the behavior of these species in aqueous solutions. However, it is important to point out that according to Carrol at al.,[39] at pressures higher than 10 bar the non-ideality of the neutral species in the aqueous solutions can no longer be neglected, and thus neutral-neutral and neutral-ions parameters are required to be added to the Pitzer equations. Likewise, the fugacity coefficients are also important to be taken into account at high pressures, and these coefficients can be easily calculated using for instance the Redlich-Kwong equations.[34]

Although the parameters in Table 2 represent interactions at 25 °C, it is not a poor approximation to use these parameters to estimate the speciation at higher temperatures. This is because, according to Silvester and Pitzer,[40,41] even 20 degrees difference in temperature is not sufficient to cause a dramatic change in the virial parameters in the Pitzer equations. This can be confirmed in Figure 2, which contains a comparison between the calculated and the experimental values[42] at 60

°C. As illustrated in this figure, there is a good match between these calculated experimental values[42] at 60 °C, which slightly deteriorates at higher concentrations.

Table 4. Comparison between calculated and experimental values[37] related to the speciation of the CO_2-NH_3-H_2O system at 25 °C.

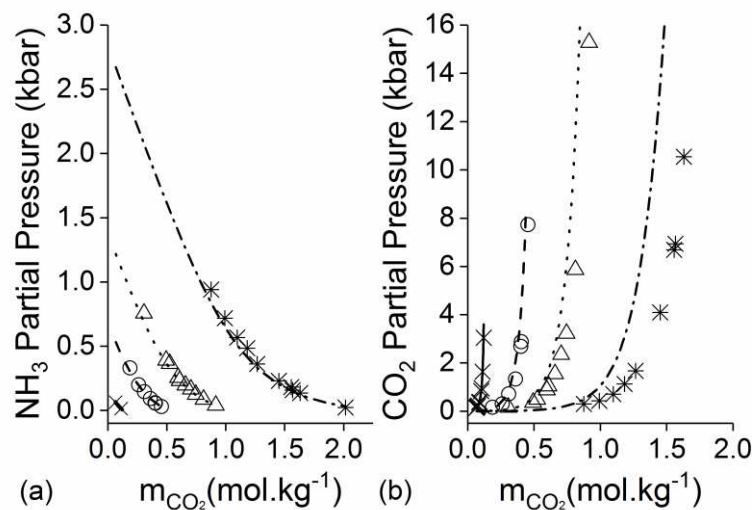| Initial Values (mol. kg^{-1})		Experimental[37] and Calculated Values (mol. kg^{-1})					
$[NH_3]_o$	$[CO_2]_o$	CO_3^{2-} experimental	CO_3^{2-} calculated	HCO_3^- experimental	HCO_3^- calculated	NH_2COOH^- experimental	NH_2COOH^- calculated
1.59	1.14	0.12	0.13	0.86	0.81	0.17	0.20
3.17	2.27	0.23	0.30	1.6	1.50	0.44	0.45
2.32	1.42	0.24	0.25	0.77	0.78	0.41	0.39
0.95	0.5	0.08	0.09	0.24	0.28	0.18	0.13
1.9	1	0.19	0.21	0.48	0.46	0.32	0.33
0.69	0.24	0.062	0.060	0.122	0.109	0.057	0.074
1.14	0.48	0.10	0.11	0.2	0.20	0.18	0.16
1.37	0.6	0.14	0.14	0.24	0.25	0.22	0.21
0.92	0.36	0.084	0.087	0.15	0.16	0.13	0.12
2.05	0.95	0.22	0.23	0.37	0.36	0.36	0.36
1.32	0.45	0.11	0.13	0.17	0.15	0.17	0.18
2.18	0.91	0.23	0.24	0.32	0.29	0.36	0.38
3.02	1.35	0.32	0.36	0.41	0.41	0.62	0.58
4	1.67	0.39	0.49	0.39	0.40	0.9	0.79
6.88	3.18	0.73	0.91	0.68	0.73	1.77	1.54
6.03	2.73	0.69	0.79	0.63	0.63	1.41	1.31
8.95	4.27	1.32	1.17	0.68	0.97	2.27	2.13

Figure 1. Comparison between experimental partial pressures[38] [×: NH_3=0.13 m, ○: NH_3=0.51 m, △: NH_3=1.03 m, ∗: NH_3=2.11 m] and calculated partial pressures [solid line: NH_3=0.13 m, dashed line: NH_3=0.51 m, dotted line: NH_3=1.03 m, dash dotted line: NH_3=2.11 m] at 20 °C: (a) NH_3 partial pressures, and (b) CO_2 partial pressures.
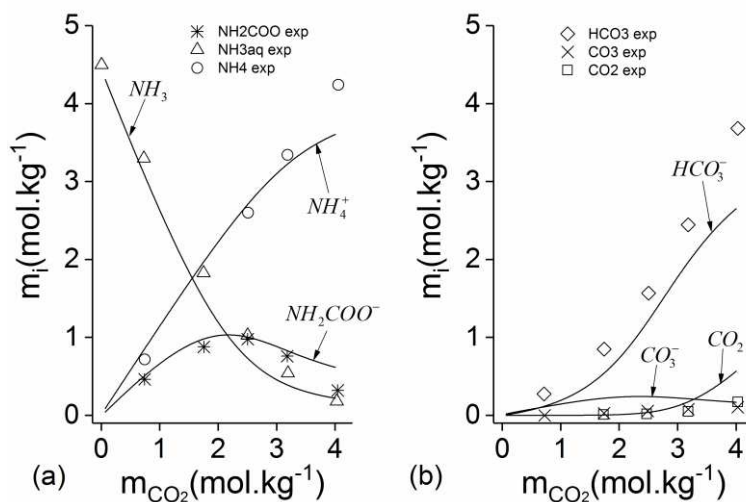

Figure 2. Chemical speciation involving the NH_3-CO_2-H_2O system at 60 °C: symbols represent experimental values[42] [△: NH_3, ○: NH_4^+, ∗: NH_2COO^-, ×: CO_3^{2-}, □: CO_2, ◊: HCO_3^-], and lines represent the calculated values [solid lines: this study]: (a) NH_3, NH_4^+ and NH_2COO^-, and (b) CO_3^{2-}, CO_2, HCO_3^-.

CO₂-MEA-H₂O System

Figure 3 illustrates the speciation involving the CO_2-MEA-H_2O system. As can be seen in this figure, both the model developed in this study and the Deshmukh-Mather model[12] provide good agreement with the speciation data obtained by Raman spectroscopy,[12] but the model developed in this study agrees, in general, better with the experimental data[12] at higher concentrations than the Deshmukh-Mather model, except for the CO_2. Nevertheless, it is important to note that the model obtained in this study is entirely based on the properties of the solution, i.e. the ionic radii and charges, whereas the Deshmukh-Mather model is a semi-empirical model that requires regressed parameters. Therefore, it is indeed remarkable that both models have similar performances at describing the speciation involving aqueous MEA. The differences between the Deshmukh-Mather model[12] and this study can be further visualized in Figure 4, which illustrates quantitatively the differences between the predictions of the two models and the experimental data from the literature.[12]

In terms of pressures, Figure 5 illustrates the good agreement between the model developed in this study and the experimental pressure data.[12] However, in general the Deshmukh-Mather model[12] agrees better with the experimental pressure data[12] than this study does. This is not unexpected since the empirical parameters in the Deshmukh-Mather model[12] were obtained using VLE data, i.e. data on the CO_2 pressure versus the CO_2 concentration in aqueous solutions.
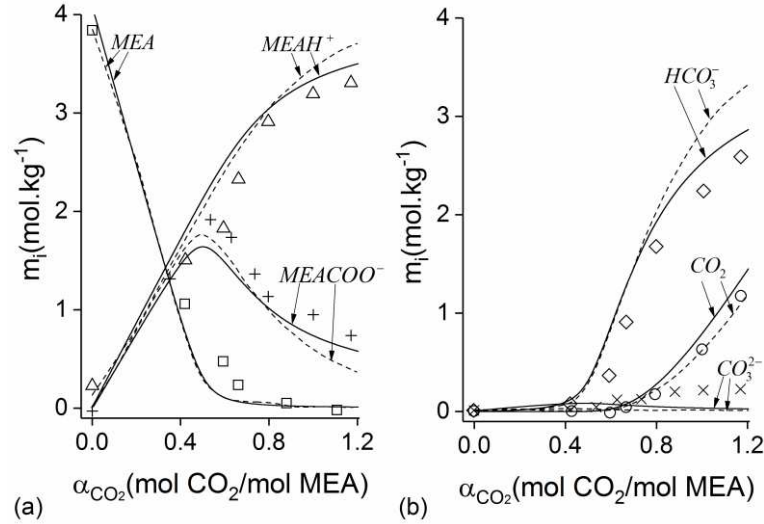
Figure 3. Chemical speciation involving the MEA-CO₂-H₂O system in 20% aqueous MEA at 40 °C: symbols represent experimental values[12] [△: $MEAH^+$, □: MEA, +: $MEACOO^-$, ×: CO_3^{2-}, O: CO_2, ◊: HCO_3^-], and lines represent calculated values [solid lines: this model, dashed lines: Deshmukh-Mather model[12]]: (a) $MEAH^+$, MEA, $MEACOO^-$, and (b) CO_3^{2-}, CO_2, HCO_3^-.
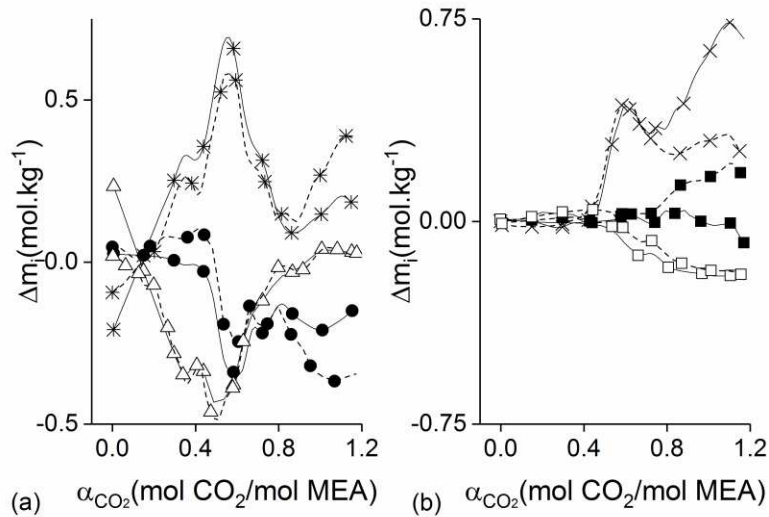

Figure 4. Residual plots between the Deshmuck-Mather model against the model developed in this study: symbols represent species [△: MEA, *: $MEAH^+$, ●: $MEACOO^-$, □: CO_3^{2-}, ■: CO_2, ×: HCO_3^-], and lines represent calculated values [solid lines: this model, dashed lines: Deshmukh-Mather model[12]]: (a) $MEAH^+$, MEA, $MEACOO^-$, and (b) CO_3^{2-}, CO_2, HCO_3^-.
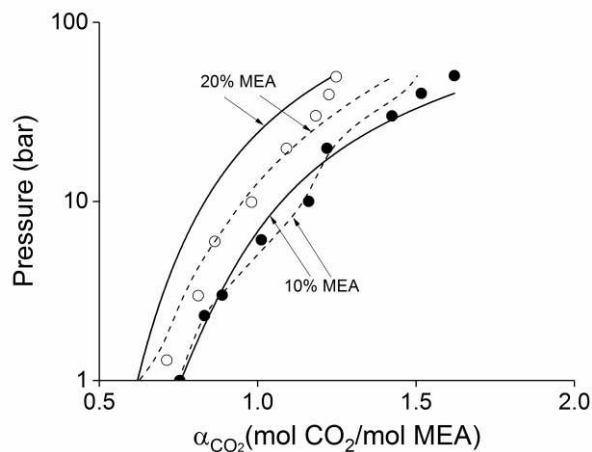
Figure 5. Total pressure as a function of the CO_2 loading at 30 °C: symbols represent experimental values[12] [●=10% aqueous MEA, ○= 20% aqueous MEA], and lines represent calculated values obtained in this study [solid line: 10% aqueous MEA, dashed line: 20% aqueous MEA].

CO_2-DEA-H_2O System

Figures 6 to 8 are examples that illustrate the good agreement between the predictions of this study and the experimental data[43] for the DEA-CO_2-H_2O system. In this case, the literature data is scarcer than in the two previous case studies. Nevertheless, the good agreement between the experimental and calculated values in both figures gives another indication of the good predictability capacity of the model presented in this study. Figure 6 shows the chemical speciation involving the DEA-CO_2-H_2O system at a temperature of 25 °C. As can be seen in this figure, the Deshmukh-Mather model[14] has also been included in the analysis, and this model predicts the carbamate with a slightly better accuracy than the model developed in this study. This slightly better agreement has been quantitatively illustrated in Figure 7, which shows the residual plots between the two models and the experimental data from the literature. In terms of the pressures, as can been seen Figure 8, both models are equally accurate in predicting the total pressures as a

16

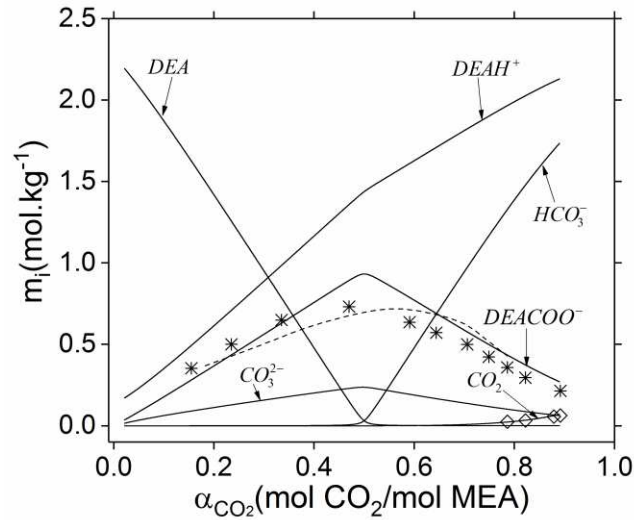function of the CO_2 loading, and have a very good agreement with the experimental data from the literature.[43]

Figure 6. Chemical speciation involving the DEA-CO_2-H_2O system in 20% aqueous DEA at 25 °C: symbols represent experimental values[43] [∗: $DEACOO^-$, ◊: CO_2], and lines represent calculated values [solid lines: this model, dashed line: Deshmukh-Mather model[14]].
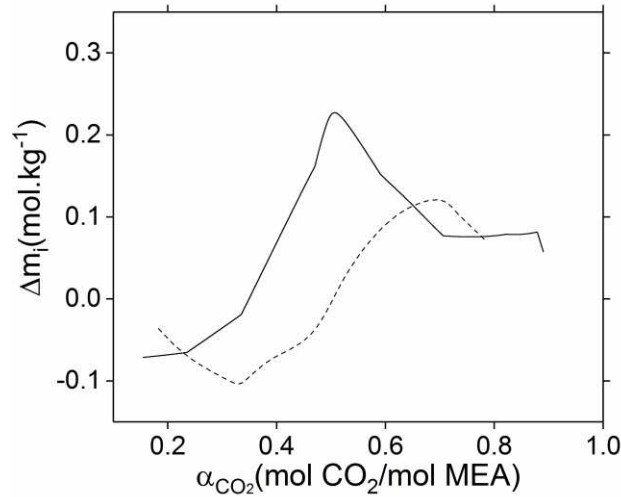

Figure 7. Residual Plots comparing the experimental values[43] from the literature and the two models investigated to describe the DEA-CO_2-H_2O system in 20% aqueous DEA at 25 °C [solid lines: this model, dashed line: Deshmukh-Mather model[14]].
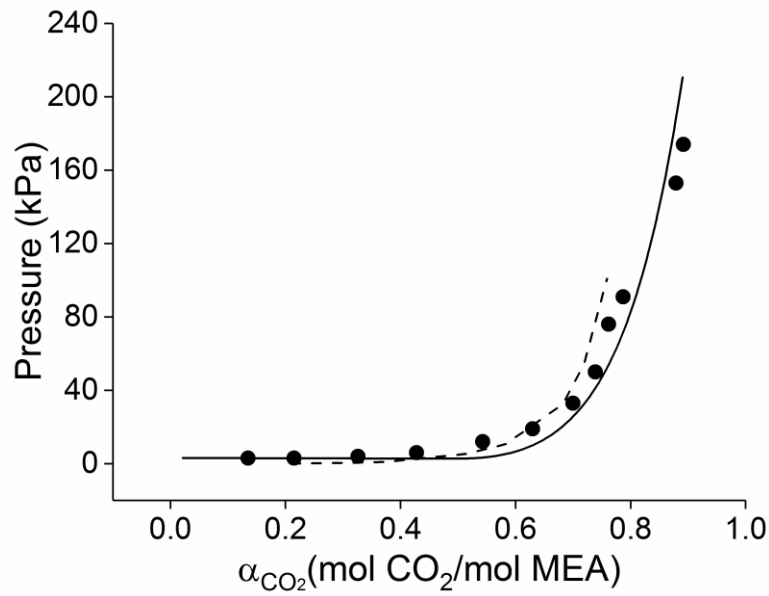
Figure 8. Total pressure as a function of the CO_2 loading at 25 °C in 20% aqueous DEA [●=experimental values[43], solid line: this model, dashed line: Deshmukh-Mather model[14]].

CONCLUSIONS

A new approach to predict the equilibrium involving CO_2 capture using chemical solvents is demonstrated in this study. In particular, the equilibrium is predicted using only the properties of the solution, i.e. the ionic radii and charges, in contrast to the models available in the literature, which require the previous knowledge of some experimental data to predict speciation. Moreover, comparison plots are provided to demonstrate the prediction abilities of the model as well as its limitations. As a conclusion, the model was able to accurately predict speciation involving chemical solvents up to a solvent mass fraction of 20%. Beyond this limit, more complex models are required.

AUTHOR INFORMATION

Corresponding Author

Dr Kevin Hughes

* Tel: +44 114 215 7214.

email: k.j.hughes@sheffield.ac.uk

ACKNOWLEDGMENT

ABBREVIATIONS

Latin Symbols

a_w, water activity

$A_{1,i}$ to $A_{4,i}$, parameters of the equation representing the temperature dependence of the equilibrium constants

$B_{MX}^{(0)}$, $B_{MX}^{(1)}$, second virial Coefficients representing short-range binary interactions

$D_{1,i}$ to $D_{5,i}$, parameters of the equation representing the temperature dependence of the Henry constants

f_w^0, the fugacity of the liquid water

$H_{i,w}^{(m)}$, Henry constant

K_i, equilibrium constant of a reaction i

m_i, molality of the component i

n, number of experimental data points

P, total pressure

I, ionic strength

r_M, ionic radii of the cation

r_{M_j}, ionic radii of the cations of a polyatomic ion

r'_{M_j}, covalent radii of the cations of a polyatomic ion

r_X, ionic radii of the anion

r_{X_k}, ionic radii of the anions of a polyatomic ion

r'_{X_k}, covalent radii of the anions of a polyatomic ion

T, temperature in Kelvin

y_i, molar fraction of a molecular solute in vapor phase

y_w, molar fraction of water in vapor phase

z_M, charge of the cation

z_X, charge of the anion

Greek Symbols

γ_i, activity coefficient of species i

ε_1, power factor that correlates the thermochemical radii of a complex anion with its ionic charge

ε_2, power factor that correlates the thermochemical radii of the complex cation with its ionic charge

ε_3, power factor that correlates the thermochemical radii of a complex cation with the ionic radii of its individual single ions

κ_1, constant that correlates the thermochemical radii of a complex cation with the ionic radii of its individual ions

φ_w, water fugacity coefficient on the vapour phase

ν_j, number of single cations of a given species

ν_k, number of single anions of a given species

Subscripts

j, number of cations

k, number of anions

M, cation

X, anion

w, water

REFERENCES

(1)   O'Neill, B. C.; Oppenheimer, M.; Warren, R.; Hallegatte, S.; Kopp, R. E.; Pörtner, H. O.; Scholes, R.; Birkmann, J.; Foden, W.; Licker, R.; et al. IPCC Reasons for Concern Regarding Climate Change Risks. *Nat. Clim. Chang.* **2017**, *7*, 28.

(2)   Pazuki, G. R.; Pahlevanzadeh, H.; Ahooei, A. M. Prediction of Phase Behavior of CO_2-NH_3-H_2O System by Using the UNIQUAC-Non Random Factor (NRF) Model. *Fluid Phase Equilib.* **2006**, *242* (1), 57.

(3)   Thomsen, K.; Rasmussen, P. Modeling of Vapor-Liquid-Solid Equilibrium in Gas-Aqueous Electrolyte Systems. *Chem. Eng. Sci.* **1999**, *54* (12), 1787.

(4)   Kurz, F.; Rumpf, B.; Maurer, G. Vapor-Liquid-Solid Equilibria in the System NH_3-CO_2-H_2O from around 310 to 470 K: New Experimental Data and Modeling. *Fluid Phase Equilib.* **1995**, *104* (C), 261.

(5)   Xu, Y.; Wang, Z.; Liu, X.; Jin, B. Modeling of the NH_3-CO_2-H_2O Vapor-Liquid Equilibria Behavior with Species-Group Pitzer Activity Coefficient Model. *Int. J. Greenh. Gas Control* **2014**, *31*, 113.

(6)   He, L.; Yu, D.; Lv, W.; Wu, J.; Xu, M. A Novel Method for CO_2 Sequestration via Indirect Carbonation of Coal Fly Ash. *Ind. Eng. Chem. Res.* **2013**, *52* (43), 15138.

(7)   Edwards, T. J.; Maurer, G.; Newman, J.; Prausnitz, J. M. Vapor-Liquid Equilibria in Multicomponent Aqueous Solutions of Volatile Weak Electrolytes. *AIChE J.* **1978**, *24*, 966.

(8)   Ahn, C. K.; Lee, H. W.; Lee, M. W.; Chang, Y. S.; Han, K.; Rhee, C. H.; Kim, J. Y.; Chun, H. D.; Park, J. M. Determination of Ammonium Salt/ion Speciation in the CO_2 Absorption Process Using Ammonia Solution: Modeling and Experimental Approaches. In *Energy Procedia*; 2011; Vol. 4, pp 541–547.

(9)   Darde, V.; Thomsen, K.; van Well, W. J. M.; Bonalumi, D.; Valenti, G.; Macchi, E. Comparison of Two Electrolyte Models for the Carbon Capture with Aqueous Ammonia. *Int. J. Greenh. Gas Control* **2012**, *8*, 61.

(10)   Pawlikowski, E. M.; Newman, J.; Prausnitz, J. M. Phase Equilibriums for Aqueous Solutions of Ammonia and Carbon Dioxide. *Ind. Eng. Chem. Process Des. Dev.* **1982**, *21*, 764.

(11)   Austgen, D. M.; Rochelle, G. T.; Peng, X.; Chen, C. C. Model of Vapor—Liquid Equilibria for Aqueous Acid Gas—Alkanolamine Systems Using the Electrolyte—NRTL Equation. *Ind. Eng. Chem. Res.* **1989**, *28* (7), 1060.

(12)   Wong, M. K.; Shariff, A. M.; Bustam, M. A. Raman Spectroscopic Study on the Equilibrium of Carbon Dioxide in Aqueous Monoethanolamine. *RSC Adv* **2016**, *6*, 10816.

(13)   Tong, D.; Trusler, J. P. M.; Maitland, G. C.; Gibbins, J.; Fennell, P. S. Solubility of Carbon Dioxide in Aqueous Solution of Monoethanolamine or 2-Amino-2-Methyl-1-Propanol: Experimental Measurements and Modelling. *Int. J. Greenh. Gas Control* **2012**, *6*, 37.

(14)   Benamor, A.; Aroua, M. K. Modeling of CO2 Solubility and Carbamate Concentration in DEA, MDEA and Their Mixtures Using the Deshmukh-Mather Model. *Fluid Phase Equilib.* **2005**, *231* (2), 150.

(15) Aronu, U. E.; Gondal, S.; Hessen, E. T.; Haug-Warberg, T.; Hartono, A.; Hoff, K. A.; Svendsen, H. F. Solubility of CO_2 in 15, 30, 45 and 60 Mass% MEA from 40 to 120°C and Model Representation Using the Extended UNIQUAC Framework. *Chem. Eng. Sci.* **2011**, *66* (24), 6393.

(16) Fan, G. J.; Wee, A. G. H.; Idem, R.; Tontiwachwuthikul, P. NMR Studies of Amine Species in MEA-CO_2-H_2O System: Modification of the Model of Vapor-Liquid Equilibrium (VLE). *Ind. Eng. Chem. Res.* **2009**, *48* (5), 2717.

(17) Arshad, M. W.; Fosbol, P. L.; Von Solms, N.; Svendsen, H. F.; Thomsen, K. Equilibrium Solubility of CO_2 in Alkanolamines. In *Energy Procedia*; 2013; Vol. 51, pp 217–223.

(18) Liu, Y.; Zhang, L.; Watanasiri, S. Representing Vapor−Liquid Equilibrium for an Aqueous MEA−CO_2 System Using the Electrolyte Nonrandom-Two-Liquid Model. *Ind. Eng. Chem. Res.* **1999**, *38* (5), 2080.

(19) Zhang, Y.; Que, H.; Chen, C. C. Thermodynamic Modeling for CO_2 Absorption in Aqueous MEA Solution with Electrolyte NRTL Model. *Fluid Phase Equilib.* **2011**, *311* (1), 67.

(20) Idris, Z.; Jens, K. J.; Eimer, D. A. Speciation of MEA-CO_2 Adducts at Equilibrium Using Raman Spectroscopy. In *Energy Procedia*; 2014; Vol. 63, pp 1424–1431.

(21) Böttinger, W.; Maiwald, M.; Hasse, H. Online NMR Spectroscopic Study of Species Distribution in MEA-H_2O-CO_2 and DEA-H_2O-CO_2. *Fluid Phase Equilib.* **2008**, *263* (2), 131.

(22) Simoes, M. C.; Hughes, K. J.; Ingham, D. B.; Ma, L.; Pourkashanian, M. Estimation of the Pitzer Parameters for 1−1, 2−1, 3−1, 4−1, and 2−2 Single Electrolytes at 25 °C. *J. Chem. Eng. Data* **2016**, *61*, 2536−2554.

(23) Simoes, M. C.; Hughes, K. J.; Ingham, D. B.; Ma, L.; Pourkashanian, M. Estimation of the

Thermochemical Radii and Ionic Volumes of Complex Ions. *Inorg. Chem.* **2017**, *56*, 7566−7573.

(24) Austgen, D. M.; Rochelle, G. T.; Chen, C.-C. Model of Vapor-Liquid Equilibria for Aqueous Acid Gas-Alkanolamine Systems. 2. Representation of H_2S and CO_2 Solubility in Aqueous MDEA and $C0_2$ Solubility in Aqueous Mixtures of MDEA with MEA or DEA. *Ind. Eng. Chem. Res.* **1991**, *30* (543–555).

(25) Pitzer, K. S. Thermodynamics of Electrolytes. I. Theoretical Basis and General Equations. *J. Phys. Chem.* **1973**, *77*, 268.

(26) Pitzer, K. S.; Mayorga, G. Thermodynamics of Electrolytes II. Activity and Osmotic Coefficients for Strong Electrolytes with One or Both Ions Univalent. *J. Phys. Chem.* **1973**, *77*, 2300.

(27) Pitzer, K. S.; Mayorga, G. Thermodynamics of Electrolytes. III. Activity and Osmotic Coefficients for 2-2 Electrolytes. *J. Solution Chem.* **1974**, *3*, 539.

(28) Pitzer, K. S.; Kim, J. J. Thermodynamics of Electrolytes. IV. Activity and Osmotic Coefficients for Mixed Electrolytes. *J. Am. Chem. Soc.* **1974**, *1426*, 5701.

(29) Pitzer, K. S. Thermodynamics of Electrolytes. V. Effects of Higher-Order Electrostatic Terms. *J. Solution Chem.* **1975**, *4*, 249.

(30) Harvie, C. E.; Møller, N.; Weare, J. H. The Prediction of Mineral Solubilities in Natural Waters: The Na-K-Mg-Ca-H-Cl-SO4-OH-HCO_3-CO_3-CO_2-H_2O System to High Ionic Strengths at 25°C. *Geochim. Cosmochim. Acta* **1984**, *48*, 723.

(31) Marcus, Y. Thermodynamics of Solvation of Ions. Part 5.-Gibbs Free Energy of Hydration at 298.15 K. *J. Chem. Soc. Faraday Trans.* **1991**, *87*, 2995.

(32) Marcus, Y. A Simple Empirical Model Describing the Thermodynamics of Hydration of

Ions of Widely Varying Charges, Sizes, and Shapes. *Biophys. Chem.* **1994**, *51*, 111.

(33)   Rumpf, B.; Weyrich, F.; Maurer, G. Enthalpy Changes upon Partial Evaporation of Aqueous Solutions Containing Ammonia and Carbon Dioxide. *Ind. Eng. Chem. Res.* **1998**, *37*, 2983.

(34)   Redlich, O.; Kwong, J. N. S. On the Thermodynamics of Solutions; an Equation of State; Fugacities of Gaseous Solutions. *Chem. Rev.* **1949**, *44* (1), 233.

(35)   Lucia, A.; Amale, A.; Taylor, R. Distillation Pinch Points and More. *Comput. Chem. Eng.* **2008**, *32* (6), 1350.

(36)   Lee, L. L. *Molecular Thermodynamics of Electrolyte Solutions*; World Scientific Publishing Co. Pte Ltd: CA, 2008.

(37)   Holmes, P. E.; Naaz, M.; Poling, B. E. Ion Concentrations in the CO_2-NH_3−H_2O System from 13 C NMR Spectroscopy. *Ind. Eng. Chem. Res.* **1998**, *37*, 3281.

(38)   Pexton, S.; Badger, E. H. M. The Examination of Aqueous Solutions Containing Only Ammonia and Carbon Dioxide. *J. Soc. Chem. Ind.* **1938**, *57*, 107.

(39)   Carroll, J. J.; Slupsky, J. D.; Mather, A. E. The Solubility of Carbon Dioxide in Water at Low Pressure. *J. Phys. Chem. Ref. Data* **1991**, *20* (6), 1201.

(40)   Silvester, L. F.; Pitzer, K. S. Thermodynamics of Electrolytes. X. Enthalpy and the Effect of Temperature on the Activity Coefficients. *J. Solution Chem.* **1978**, *7*, 327.

(41)   Simoes, M. C.; Hughes, K. J.; Ingham, D. B.; Ma, L.; Pourkashanian, M. Temperature Dependence of the Parameters in the Pitzer Equations. *J. Chem. Eng. Data* **2017**, *62*, 2000−2013.

(42)   Lichtfers, U.; Rump, B. Infrarotspektroskopische Untersuchungen Zur Ermittlung von Spezieskonzentrationen in Wassrigen Losungen, Die Ammoniak Und Kohlendioxid

Enthalten. *Chemie Ing. Tech.* **2000**, *72*, 1526.

(43)   Diab, F.; Provost, E.; Laloué, N.; Alix, P.; Souchon, V.; Delpoux, O.; Fürst, W. Quantitative
Analysis of the Liquid Phase by FT-IR Spectroscopy in the System CO_2/diethanolamine
(DEA)/H_2O. *Fluid Phase Equilib.* **2012**, *325*, 90.

TOC GRAPHIC